Asociación Argentina
de Mecánica Computacional

Mecánica Computacional Vol XXIX, págs. 3891-3907 (artículo completo)
Eduardo Dvorkin, Marcela Goldschmit, Mario Storti (Eds.)
Buenos Aires, Argentina, 15-18 Noviembre 2010

CALIBRATION OF ANALYTICAL SOLUTIONS TO PROBLEMS OF POLLUTANT DISPERSION IN THE SURF ZONE

Bruno S. Solheid[1], **Maurício F. Gobbi**[1] **and Andre J. Torii**[1]

[1]*Programa de Pós-graduação em Métodos Numéricos em Engenharia, Universidade Federal do Paraná, Rua Cel. Francisco Heráclito dos Santos 100, Jardim das Américas, Curitiba,* *http://www.ufpr.br/portal/*

Keywords: Surf Zone, Analytical Solution, Dispersion of pollutants.

Abstract.

This work presents an example from a methodology for building mathematical expressions, who describe the behaviors of the dispersion of pollutants in the surf zone. This methodology is based in calibration of analytical solutions from the diffusion-advection equation. Simple cases of dispersion were defined mathematically, then solved by classical mathematical methods, such integral transforms and similarity solutions. Then the analytical solutions were calibrated by an optimization technique, to fit the results of a more complex dispersion case, that was solved numerically in other work.

Copyright © 2010 Asociación Argentina de Mecánica Computacional http://www.amcaonline.org.ar

1 INTRODUCTION

In the coast of Paraná, the environmental problems of an inadequate human occupation, has already been observed from a long time. The paper (Angulo, 1984) deals with the erosion and pollution of coastal waters of Paraná. In the last years the pollution of coastal waters of Paraná by pathogens reached a critical level. An example of this situation was the results of the balneability analysis of the coastal waters of Paraná in the season of 2008/2009 in which only nine of forty-three points were considered suitable for bathing.

In the state of Paraná the policy of balneability is based on the resolution 274/2000 of CONAMA (Conselho Nacional do Meio Ambiente) and works as follows: water samples are collected in the critical zones, the samples are analyzed for the presence of pathogens. If the presence of pathogens is below the maximum permissible concentration in eighty percent of the samples, then the area are suitable for swimming. Otherwise the area is interdicted in a neighborhood of 200 meters centered in the sample point.

The estimation of the size of banned area around a point of contamination is the initial motivation of this work. Besides the size of banned area, another practical issue is the necessity of make decisions in a short time. To deal with those issues the proposal of this work is to present a methodology for building mathematical expressions that are able to replicate some results of complex dispersion problems in the surf zone, modeled numerically

2 ANALITYCAL SOLUTIONS FOR DISPERSION PROBLEMS WITH FIRST ORDER DECAY

In this section will be build some analytical solutions to the problem of transport of scalar. Particular cases of these solutions will be calibrated to simulate the behavior of the dispersion of more complex cases.

2.1 Pollution load entering a clean system

The problem considered below represents the behavior of the mean concentration (in the water column) of a scalar such that your diffusivity coefficient is isotropic and is denoted by D. The mean concentration is denoted by C. In the initial time there is no concentration of the scalar in the medium i.e $C(x, y, 0) = 0$. The fluid that compose the medium is subject to a flow defined by the homogeneous velocities U and V. The scalar have a first order decay of intensity K. By physical considerations it is appropriate that the concentration tends to zero in regions far from the pollution load. The problem is put mathematically as

$$\frac{\partial C}{\partial t} + V\frac{\partial C}{\partial y} + U\frac{\partial C}{\partial x} = D\nabla^2 C - KC + Q(x, y, t) \qquad (x, y) \in \mathbb{R}^2, t \in (0, \infty); \tag{1}$$

$$\lim_{|x|\to\infty} C(x, y, t) = 0; \tag{2}$$

$$\lim_{|y|\to\infty} C(x, y, t) = 0; \tag{3}$$

$$C(x, y, 0) = 0 \tag{4}$$

Copyright © 2010 Asociación Argentina de Mecánica Computacional http://www.amcaonline.org.ar

By the conditions (2) and (3) and imposing restrictions on the forcing term $Q(x,y,t)$ is reasonable to assume that

$$\int_{-\infty}^{\infty}\int_{-\infty}^{\infty} \mid C(x,y,t) \mid dxdy < \infty. \tag{5}$$

By (5) it is possible to apply the double Fourier transform in (1). Because the condition (4), there are the possibility of apply the Laplace transform in in (1). Putting together the Fourier and Laplace transforms we define the composite transform

$$\mathcal{T}\left\{f(x,y,t)\right\} = \int_{0}^{\infty}\int_{-\infty}^{\infty}\int_{-\infty}^{\infty} \exp[-st - i\omega_1 x - i\omega_2 y] f(x,y,t)dxdydt. \tag{6}$$

Applying $\mathcal{T}$ in (1) and considering $\mathcal{T}\left\{Q(x,y,t)\right\} = \overline{\widehat{Q}}(\omega_1,\omega_2,s)$, $\mathcal{L}\{f(t)\} = \overline{f}(s)$ and $\mathcal{T}\{C(x,y,t)\} = \Psi(\omega_1,\omega_2,s)$ we get the follow expression

$$s\Psi - \widehat{C}(\omega_1,\omega_2,0) + i\omega_1 U\Psi + i\omega_2 V\Psi = D(-\omega_1^2 - \omega_2^2)\Psi - K\Psi + \overline{\widehat{Q}}(\omega_1,\omega_2,s), \tag{7}$$

where,

$$\widehat{C}(\omega_1,\omega_2,t) = \int_{-\infty}^{\infty}\int_{-\infty}^{\infty} \exp[-i\omega_1 x - i\omega_2 y] C(x,y,t)dxdy. \tag{8}$$

By (4) it is possible to express (7) as

$$\Psi(\omega_1,\omega_2,s) = \frac{1}{(s + i\omega_1 U + i\omega_2 V + D\omega_1^2 + D\omega_2^2 + K)}\overline{\widehat{Q}}(\omega_1,\omega_2,s). \tag{9}$$

To get the solution of the problem, now we must apply the inverse transform $\mathcal{T}^{-1}$ on (9). It is possible to demonstrate that

$$\mathcal{T}^{-1} = \mathcal{L}^{-1} \circ \mathcal{F}_x^{-1} \circ \mathcal{F}_y^{-1}, \tag{10}$$

where, $\circ$ represents the operation of composition, $\mathcal{L}^{-1}$ is the inverse Laplace transform, $\mathcal{F}_x^{-1}$ is the inverse Fourier transform in x and $\mathcal{F}_y^{-1}$ is the inverse Fourier transform in y.

Applying $\mathcal{L}^{-1}$ on (9)and considering the Laplace's convolution and translation properties we have

$$\mathcal{L}^{-1}\left\{\Psi\right\} = \int_0^t \exp\left[-A(t-\tau)\right]\widehat{Q}(\omega_1,\omega_2,\tau)d\tau, \tag{11}$$

where $A = (Ui\omega_1 + Vi\omega_2 + D(\omega_2^2 + \omega_1^2) + K)$. Applying the inverse Fourier transform in x in the equation (11), by the convolution theorem and by the Fubini's theorem (Figueiredo, 1977) we have

$$\mathcal{F}_x^{-1}\left\{\mathcal{L}^{-1}\left\{\Psi\right\}\right\} = \int_0^t \mathcal{F}^{-1}\left\{\exp\left[-A(t-\tau)\right]\right\} * \mathcal{F}^{-1}\left\{\widehat{Q}(\omega_1,\omega_2,\tau)\right\} d\tau. \tag{12}$$

Copyright © 2010 Asociación Argentina de Mecánica Computacional http://www.amcaonline.org.ar

Solving the inverse Fourier transform in (12) we have

$$\mathcal{F}_x^{-1}\left\{\mathcal{L}^{-1}\left\{\Psi\right\}\right\} = \int_0^t \int_{-\infty}^{\infty} \widehat{Q}(\xi,\omega_2,\tau)\exp[B]\times \\ \times\frac{\exp\left[\frac{-(x-\xi-U(t-\tau))^2}{4D(t-\tau)}\right]}{2\sqrt{D\pi(t-\tau)}}d\xi d\tau \tag{13}$$

where $B = Vi\omega_2 - D\omega_2^2(t-\tau) - K(t-\tau)$. Applying the inverse Fourier transform in y in the expression (13) we have

$$C(x,y,t) = \int_0^t \int_{-\infty}^{\infty} \mathcal{F}_y^{-1}\left\{\widehat{Q}(\xi,\omega_2,\tau)\exp[-Vi\omega_2 - D\omega_2^2(t-\tau) - K(t-\tau)]\right\}\times \\ \times\frac{\exp\left[\frac{-(x-\xi-U(t-\tau))^2}{4D(t-\tau)}\right]}{2\sqrt{D\pi(t-\tau)}}d\xi d\tau \tag{14}$$

Repeatedly using the convolution theorem, the linearity of the inverse fourier transform and the Fubini's theorem we have

$$C(x,y,t) = \int_0^t \int_{-\infty}^{\infty}\int_{-\infty}^{\infty} Q(\xi,\lambda,\tau)\frac{\exp\left[-K(t-\tau) - \frac{(y-\lambda-V(t-\tau))^2}{4D(t-\tau)}\right]}{2\sqrt{D\pi(t-\tau)}}\times \\ \times\frac{\exp\left[\frac{-(x-\xi-U(t-\tau))^2}{4D(t-\tau)}\right]}{2\sqrt{D\pi(t-\tau)}}d\lambda d\xi d\tau \tag{15}$$

Finally, the solution is given by

$$C(x,y,t) = \int_0^t \int_{-\infty}^{\infty}\int_{-\infty}^{\infty} \frac{Q(\xi,\lambda,\tau)}{4D\pi(t-\tau)}\exp\left[-K(t-\tau) - \frac{(y-\lambda-V(t-\tau))^2}{4D(t-\tau)}\right]\times \\ \times\exp\left[-\frac{(x-\xi-U(t-\tau))^2}{4D(t-\tau)}\right]d\lambda d\xi d\tau \tag{16}$$

2.2 Pollutants in a region with a physical barrier

This problem is similar to the problem presented on the last section, but in this case there is a barrier in the $x = 0$ axis. The mathematical formulation of this problem is intended to describe the behavior of the scalar dispersion in a medium with a physical barrier. The problem is given by

$$\frac{\partial C}{\partial t} + V\frac{\partial C}{\partial y} = D\nabla^2 C - KC + Q(x,y,t) \qquad (x,t)\in(0,\infty), \qquad y\in(-\infty,\infty); \tag{17}$$

and the conditions

$$\lim_{y\to\infty} C(x,y,t) = 0; \tag{18}$$

Copyright © 2010 Asociación Argentina de Mecánica Computacional http://www.amcaonline.org.ar

$$\lim_{x\to\infty} C(x,y,t) = 0; \tag{19}$$

$$C(x,y,0) = 0; \tag{20}$$

$$\frac{\partial C(0,y,t)}{\partial x} = 0. \tag{21}$$

To deal with the condition (21) the image method can be used. First we must to analyze the solution when we extend the domain to the $(-\infty, \infty)$ in x axis. In the extended domain the equation is decomposed in two parts, the even and odd parts relative to the $x = 0$ axis. When we extend the solution we also need to extend the forcing term $Q(x,y,t)$. So the solution have the form

$$C(x,y,t) = S(x,y,t) + A(x,y,t), \tag{22}$$

where

$$S(x,-y,t) = S(x,y,t); \tag{23}$$

$$A(x,-y,t) = -A(x,y,t). \tag{24}$$

Applying (22) in (17), we have

$$\frac{\partial(S+A)}{\partial t} + U\frac{\partial(S+A)}{\partial x} = D\nabla^2(S+A) - K(S+A) + Q_{ext}(x,y,t). \tag{25}$$

Let E1 and E2, be even functions and O1 and O2, be odd functions, then

$$E1 + O1 = E2 + O2 \rightarrow E1 = E2 \text{ and } O1 = O2 \tag{26}$$

Using the relation (26) we can separate the expression (25) and the initial an boundary conditions in the even and odd parts. Like the solution, the forcing term is also separated in the even and odd parts, who is denoted respectively by: $sQ_{ext}(x,y,t)$ and $aQ_{ext}(x,y,t)$. With that we can separate the problem in two parts. The even problem:

$$\frac{\partial S}{\partial t} + V\frac{\partial S}{\partial y} = D\nabla^2 S - KS + sQ_{ext}(x,y,t) \qquad (x,y) \in \mathbb{R}^2, t \in (0,\infty); \tag{27}$$

$$\lim_{|x|\to\infty} S(x,y,t) = 0; \tag{28}$$

$$\lim_{|y|\to\infty} S(x,y,t) = 0; \tag{29}$$

$$S(x,y,0) = 0. \tag{30}$$

And the odd problem:

$$\frac{\partial A}{\partial t} + V\frac{\partial A}{\partial y} = D\nabla^2 A - KA + aQ_{ext}(x,y,t) \qquad (x,y) \in \mathbb{R}^2, t \in (0,\infty); \tag{31}$$

Copyright © 2010 Asociación Argentina de Mecánica Computacional http://www.amcaonline.org.ar

$$\lim_{|x|\to\infty} A(x,y,t) = 0; \tag{32}$$

$$\lim_{|y|\to\infty} A(x,y,t) = 0; \tag{33}$$

$$A(x,y,0) = 0. \tag{34}$$

When we extend the problem about the $x = 0$ axis, it is possible to extend the forcing term arbitrarily. If the forcing term is symmetrical to the $x = 0$ axis, then $aQ_{ext}(x,y,t) = 0$ and the anti-symmetric problem only have the trivial solution. As consequence the solution to the original problem have the form $C(x,y,t) = S(x,y,t)$ and consequently the condition (21) will be met. Making Q_{ext} symmetric, we have the problem in the extended domain

$$\frac{\partial C}{\partial t} + V\frac{\partial C}{\partial y} = D\nabla^2 C - KC + Q_{ext}(x,y,t) \qquad (x,y) \in \mathbb{R}^2, t \in (0,\infty); \tag{35}$$

$$\lim_{|x|\to\infty} C(x,y,t) = 0; \tag{36}$$

$$\lim_{|y|\to\infty} C(x,y,t) = 0; \tag{37}$$

$$C(x,y,0) = 0. \tag{38}$$

The solution to the problem (32)-(35) is identical to the problem (1)-(4), but in this case we have $U = 0$. Its is possible to demonstrate that the solution for the problem (35)-(38) restricted to the original domain, meets all the boundary conditions and the differential equation of the original problem.

2.3 Evolution of a concentration prescribed on the boundary

In this case the domain is semi-infinite in x and y. The concentration C is prescribed on the boundary $y = 0$. On the boundary $x = 0$ there is a physical barrier. The fluid have only v velocity. The problem is given by

$$\frac{\partial C}{\partial t} + V\frac{\partial C}{\partial y} = D\nabla^2 C - KC \qquad (y,x) \in (0,\infty), 0 < t < \infty); \tag{39}$$

$$\lim_{x\to\infty} C(x,y,t) = 0; \tag{40}$$

$$\lim_{y\to\infty} C(x,y,t) = 0; \tag{41}$$

$$C(x,0,t) = C_0(x,t); \tag{42}$$

$$C(x,y,0) = 0; \tag{43}$$

$$\frac{\partial C(0,y,t)}{\partial x} = 0. \tag{44}$$

Copyright © 2010 Asociación Argentina de Mecánica Computacional http://www.amcaonline.org.ar

To deal with the condition (44) we can use the image method. It is possible to check that the extended problem in the $x = 0$ axis, together with the function C_{0ext} being symmetric to the $x = 0$ axis, in the original domain meets all the conditions of the original problem. The extended problem is defined by

$$\frac{\partial C}{\partial t} + V\frac{\partial C}{\partial y} = D\nabla^2 C - KC \qquad (y,t) \in (0,\infty), -\infty < x < \infty); \tag{45}$$

$$\lim_{|x|\to\infty} C(x,y,t) = 0; \tag{46}$$

$$\lim_{y\to\infty} C(x,y,t) = 0; \tag{47}$$

$$C(x,0,t) = C_{0ext}(x,t); \tag{48}$$

$$C(x,y,0) = 0; \tag{49}$$

To solve this problem, we use the compose of the Laplace and Fourier transform, the transform is given by

$$\mathcal{T}\left\{f(x,t)\right\} = \int_0^\infty \int_{-\infty}^\infty \exp[-st - i\omega x] f(x,t)dxdt = \overline{\widehat{f}}(\omega,s). \tag{50}$$

Applying $\mathcal{T}$ in (45), we have

$$s\overline{\widehat{C}} - \widehat{C}(x,\omega,0) + V\frac{\partial\overline{\widehat{C}}}{\partial y} - D\frac{\partial^2\overline{\widehat{C}}}{\partial^2 y} + A\overline{\widehat{C}} = 0. \tag{51}$$

Where $A = \omega^2 D + K$. Due the condition (49), the expression (51 can by written as

$$\frac{\partial^2\overline{\widehat{C}}}{\partial^2 y} - \frac{V}{D}\frac{\partial\overline{\widehat{C}}}{\partial y} - \frac{(s-A)}{D}\overline{\widehat{C}} = 0. \tag{52}$$

The general solution from the equation (52) is given by

$$\begin{aligned}\overline{\widehat{C}}(\omega,y,s) = C1\exp\left[\left(\frac{V}{D} + \sqrt{\frac{V^2}{D^2} + \frac{4(s+A)}{D}}\right)\frac{y}{2}\right] + \\ +C2\exp\left[\left(\frac{V}{D} - \sqrt{\frac{V^2}{D^2} + \frac{4(s+A)}{D}}\right)\frac{y}{2}\right]\end{aligned} \tag{53}$$

Applying $\mathcal{T}$ in the conditions (47) and (48) we have

$$\lim_{y\to\infty} \overline{\widehat{C}}(\omega,y,s) = 0; \tag{54}$$

$$\overline{\widehat{C}}(\omega,0,s) = \overline{\widehat{C}}_{0ext}(\omega,s). \tag{55}$$

Copyright © 2010 Asociación Argentina de Mecánica Computacional http://www.amcaonline.org.ar

By (54) and (55) the expression (53) can by written as

$$\overline{\widehat{C}} = \overline{\widehat{C}}_{0ext}(\omega, s) \exp\left[\ \frac{V}{D} - \sqrt{\frac{V^2}{D^2} + \frac{4(s+A)}{D}}\right) \frac{y}{2}\right]. \tag{56}$$

After performing algebraic manipulations, the equation (56) can by written as

$$\overline{\widehat{C}} = \exp\left[\frac{Vy}{2D}\right]\overline{\widehat{C}_{0ext}}(\omega, s) \exp\left[\frac{-y}{\sqrt{D}}\sqrt{(\frac{V^2}{4D} + A + s)}\right]. \tag{57}$$

To obtain the solution we must turn back to the original variables by the inverse transform. It is possible to check that $\mathcal{T}^{-1} = \mathcal{L}^{-1} \circ \mathcal{F}_x^{-1}$. The solution is given by

$$C(x,y,t) = \mathcal{T}^{-1}\left\{\exp\left[\frac{Vy}{2D}\right]\overline{\widehat{C}_{0ext}}(\omega, s) \exp\left[\frac{-y}{\sqrt{D}}\sqrt{(\frac{V^2}{4D} + A + s)}\right]\right\} \tag{58}$$

Applying the inverse laplace transform in (57), by the convolution theorem we have

$$\widehat{C}(\omega, y, t) = \exp\left[\frac{Vy}{2D}\right]\widehat{C_{0ext}}(\omega, t) * \mathcal{L}^{-1}\left\{\exp\left[\frac{-y}{\sqrt{D}}\sqrt{(\frac{V^2}{4D} + A + s)}\right]\right\}. \tag{59}$$

Knowing that

$$\mathcal{L}\left\{\frac{l \exp\left[\frac{-l^2}{4t}\right]}{2\sqrt{\pi t^3}}\right\} = \exp -l\sqrt{s} \tag{60}$$

it is possible to use the translation theorem to find the inverse from the right side of the equation (59).

$$\mathcal{L}^{-1}\left\{\exp\left[\frac{-y}{\sqrt{D}}\sqrt{(\frac{V^2}{4D} + A + s)}\right]\right\} = \frac{y \exp\left[-\left(\frac{V^2}{4D} + A\right)t + \frac{-y^2}{4Dt}\right]}{2\sqrt{D\pi t^3}} \tag{61}$$

Putting (61) in (59)

$$\widehat{C}(\omega, y, t) = \exp\left[\frac{Vy}{2D}\right]\int_0^t \widehat{C_{0ext}}(\omega, t)\frac{y \exp\left[-\left(\frac{V^2}{4D} + A\right)(t-\tau) + \frac{-y^2}{4D(t-\tau)}\right]}{2\sqrt{D\pi(t-\tau)^3}} d\tau. \tag{62}$$

By the properties of the inverse Fourier transform and by the Fubini's theorem, we have the following relation:

$$C(x, y, t) = \exp\left[\frac{Vy}{2D}\right]\int_0^t \mathcal{F}^{-1}\left\{\widehat{C_{0ext}}(\omega, t)\frac{y \exp\left[-\left(\frac{V^2}{4D} + A\right)(t-\tau) + \frac{-y^2}{4D(t-\tau)}\right]}{2\sqrt{D\pi(t-\tau)^3}}\right\} d\tau. \tag{63}$$

Copyright © 2010 Asociación Argentina de Mecánica Computacional http://www.amcaonline.org.ar

For simplify the notation, we call Φ the argument from the inverse transform in (63). By convolution theorem we have

$$\mathcal{F}^{-1}(\Phi) = C_0(x,t)_{ext} * \mathcal{F}^{-1}\left\{ \frac{y \exp\left[-\left(\frac{V^2}{4D}+A\right)(t-\tau)+\frac{-y^2}{4D(t-\tau)}\right]}{2\sqrt{D\pi(t-\tau)^3}} \right\} \tag{64}$$

It follows that

$$\begin{aligned} &\mathcal{F}^{-1}\left\{ \frac{y \exp\left[-\left(\frac{V^2}{4D}+A\right)(t-\tau)+\frac{-y^2}{4D(t-\tau)}\right]}{2\sqrt{D\pi(t-\tau)^3}} \right\} = \\ &= \frac{y \exp\left[-\left(\frac{V^2}{4D}\right)(t-\tau)+\frac{-y^2}{4D(t-\tau)}\right]}{2\sqrt{D\pi(t-\tau)^3}} \mathcal{F}^{-1}\left\{\exp -A(t-\tau)\right\} \end{aligned} \tag{65}$$

Putting A in (65):

$$\mathcal{F}^{-1}\left\{\exp\left[-A(t-\tau)\right]\right\} = \mathcal{F}^{-1}\left\{\exp\left[-(\omega^2 D + k)(t-\tau)\right]\right\}; \tag{66}$$

$$\mathcal{F}^{-1}\left\{\exp\left[-(\omega^2 D + k)(t-\tau)\right]\right\} = \exp\left[-k(t-\tau)\right]\mathcal{F}^{-1}\left\{\exp\left[-\omega^2 D(t-\tau)\right]\right\}; \tag{67}$$

$$\mathcal{F}^{-1}\left\{\exp\left[-(\omega^2 D)(t-\tau)\right]\right\} = \frac{\exp\left[\frac{-x^2}{4(t-\tau)D}\right]}{2\sqrt{(t-\tau)D\pi}}. \tag{68}$$

Putting (64)-(68) in (63) we finally have the solution

$$\begin{aligned} C(x,y,t) = \exp\left[\frac{Vy}{2D}\right] \int_0^t \int_{-\infty}^{+\infty} C_{0ext}(\xi,\tau) \times \\ \times \frac{y \exp\left[-\left(\frac{V^2}{4D}\right)(t-\tau)+\frac{-y^2}{4D(t-\tau)}+\frac{-(x-\xi)^2}{4(t-\tau)D}-K(t-\tau)\right]}{4D\pi(t-\tau)^2} d\xi d\tau \end{aligned} \tag{69}$$

3 PARTICULAR CASES AND IMPOSITION OF CALIBRATION PARAMETERS

With the solutions presented in the last section it is possible to construct mathematical expressions through particular cases. These expressions have calibration parameters, who will be used to approximate the behavior of scalar dispersion of more complex cases, solved numerically.

3.1 Constant concentration in a line parallel to the coast

Is this section we want to begin with the solution given by the expression (69) and through simplification, obtain a simple expression who will be easy to calibrate posteriorly.

By physical considerations it is reasonable to presume that, if

$$\frac{\partial C_0(x,t)}{\partial x} = 0 \qquad \forall x \in (0,\infty), \tag{70}$$

Copyright © 2010 Asociación Argentina de Mecánica Computacional http://www.amcaonline.org.ar

then

$$\frac{\partial C(x,y,t)}{\partial x} = 0. \tag{71}$$

So, with we put $C_0(x,t) = C_0$ constant, it's expected that the final solution don't depend on x. Putting $C_0(x,t) = C_0$ in (69) we have

$$C(x,y,t) = \exp\left[\frac{Vy}{2D}\right] \int_0^t \int_{-\infty}^{+\infty} C_0 \times \\ \times \frac{y \exp\left[-\left(\frac{V^2}{4D}\right)(t-\tau) + \frac{-y^2}{4D(t-\tau)} + \frac{-(x-\xi)^2}{4(t-\tau)D} - K(t-\tau)\right]}{4D\pi(t-\tau)^2} d\xi d\tau \tag{72}$$

Assuming that the function under the integration sign, respect the conditions given by the Fubini's theorem, then (72) may be written as

$$C(x,y,t) = \exp\left[\frac{Vy}{2D}\right] \int_0^t C_0 \frac{y \exp\left[-\left(\frac{V^2}{4D}\right)(t-\tau) + \frac{-y^2}{4D(t-\tau)} - K(t-\tau)\right]}{4D\pi(t-\tau)^2} \times \\ \times \int_{-\infty}^{+\infty} \exp\left[\frac{-(x-\xi)^2}{4(t-\tau)D}\right] d\xi d\tau \tag{73}$$

The expression (73) may be written as

$$C(x,y,t) = \exp\left[\frac{Vy}{2D}\right] \int_0^t C_0 \frac{y \exp\left[-\left(\frac{V^2}{4D}\right)(t-\tau) + \frac{-y^2}{4D(t-\tau)} - K(t-\tau)\right]}{4D\pi(t-\tau)^2} \times \\ \times 2\sqrt{D(t-\tau)\pi} d\tau \tag{74}$$

The expression (73) may be written as

$$C(x,y,t) = yC_0 \exp\left[\frac{Vy}{2D}\right] \int_0^t \frac{\exp\left[-\left(\frac{V^2}{4D}\right)(t-\tau) + \frac{-y^2}{4D(t-\tau)} - K(t-\tau)\right]}{2\sqrt{D\pi(t-\tau)^3}} d\tau \tag{75}$$

To obtain an even simpler expression, we can compute the solution of the permanent problem. For this, it's necessary to solve the integral (75) with the time tending to infinity.

$$C(x,y,t) = yC_0 \exp\left[\frac{Vy}{2D}\right] \int_0^\infty \frac{\exp\left[-\left(\frac{V^2}{4D}\right)(t-\tau) + \frac{-y^2}{4D(t-\tau)} - K(t-\tau)\right]}{2\sqrt{D\pi(t-\tau)^3}} d\tau \tag{76}$$

The integral (76) have the follow solution depending on y:

$$C(y) = C_0 \exp\left[\frac{Vy}{D} - \sqrt{\frac{V^2}{D^2} + \frac{4K}{D}} y\right]. \tag{77}$$

Copyright © 2010 Asociación Argentina de Mecánica Computacional http://www.amcaonline.org.ar

4 NUMERICAL MODELING FOR DISPERSION OF COLIFORMS IN MATINHOS BEACH

This section briefly presents the results for dispersion of coliforms, given by a numerical model. The model simulate the entrance of a polluted effluent in a beach. As an example we use the characterists of the mouth of Matinhos River in the coast of Paraná.

The numerical model uses the finite difference technique for solve the diffusion-advection equation. The hydrodynamic data used in the model were generated by a Boussinesq wave model. For more details about the numerical model and the Boussinesq wave model used in this work, see Solheid (2010), Wei et al. (1995), Kennedy et al. (2000) e Chen et al. (2000).

To characterize the Matinhos River mouth, the wave model used as input:a bathymetry similar to the region and the wave characteristics of the region (have height, frequency and angle of incidence with the coast).

The figures (1)-(6) shows the concentration of coliforms given in 1000NMP(100ml)$^{-1}$, calculated through the numerical model. In all the figures "longshore" represents the axis parallel to the coast, and "crosshore" represents the axis normal to the coast. The surf zone begins approximately in 300 m.

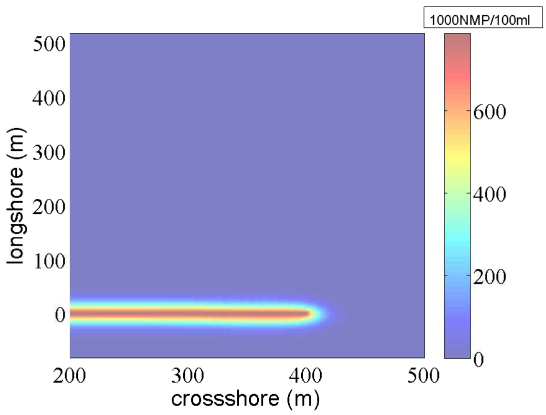

Figure 1: Numerical Simulation *t*=10min

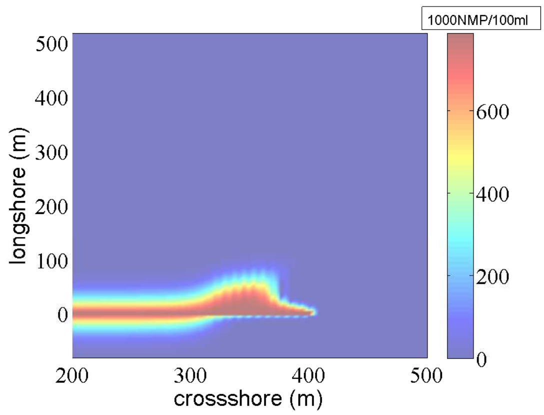

Figure 2: Numerical Simulation *t*=30min

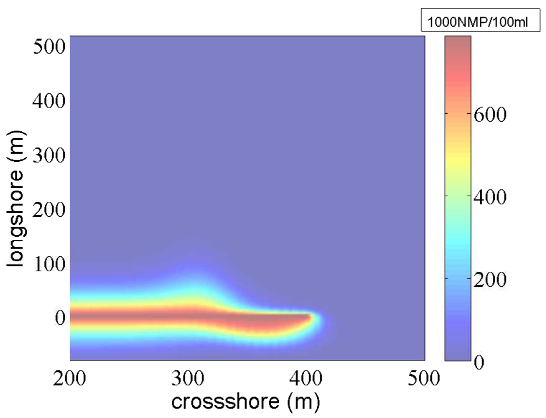

Figure 3: Numerical Simulation *t*=60min

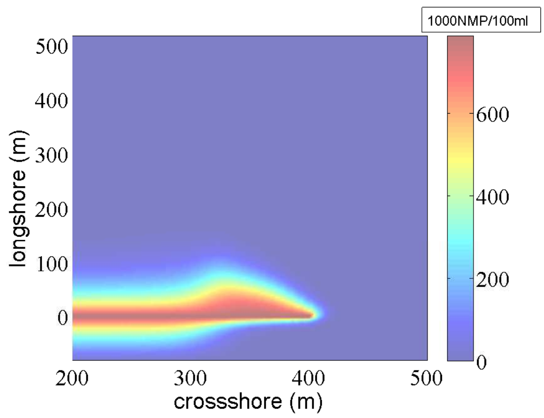

Figure 4: Numerical Simulation *t*=120min

At different times a profile of mean concentration as calculated on the surf zone along the coast. The interval used to calculate the mean values was 300 to 400 meters along the *crossshore*

Copyright © 2010 Asociación Argentina de Mecánica Computacional http://www.amcaonline.org.ar

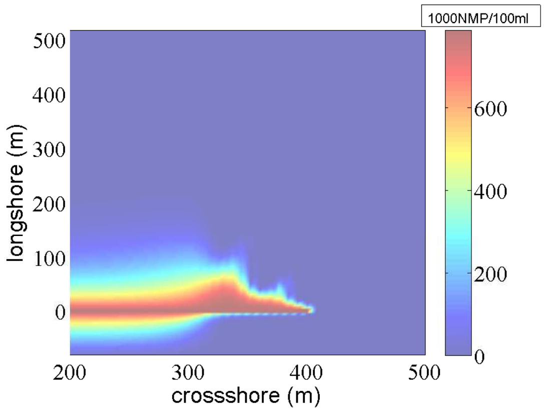

Figure 5: Numerical Simulation t=310min

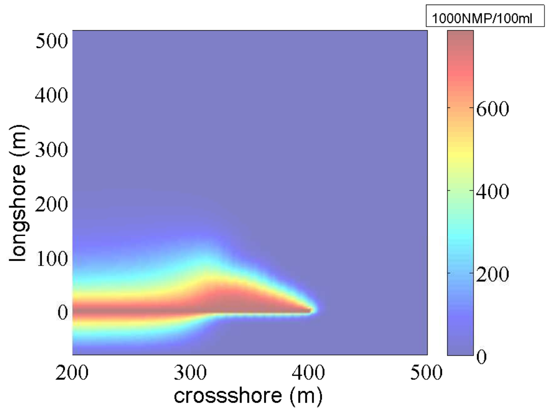

Figure 6: Numerical Simulation t=560min

axis. The figures (7) and (8) shows the profile of the mean concentration in 1000NMP(100ml)$^{-1}$ along the coast (*longshore* axis) considering that the beginning of the y axis, is the point of the river mouth.

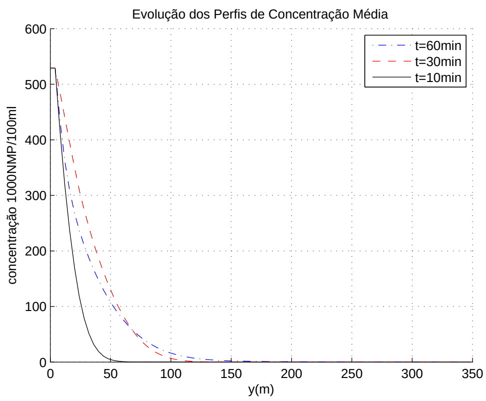

Figure 7: Mean concentration of coliform on the surf zone along the coast in t=10 min, t=30 min e t=60 min

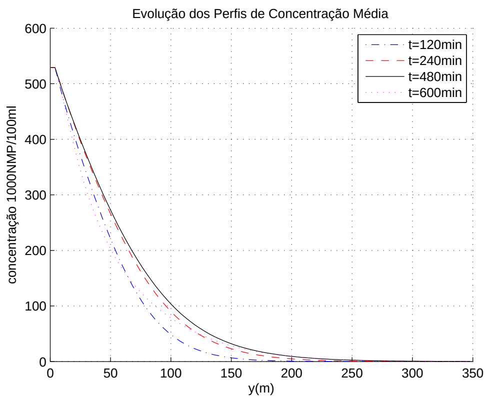

Figure 8: Mean concentration of coliform on the surf zone along the coast in t=120 min, t=240 min ,t=480 min e t=600min

Along the coast the maximum concentration in the surf zone was calculated. The interval used to calculate the maximum values was 300 to 400 meters along the *crossshore* axis. The pictures (9) and (10) shows the profiles of maximum concentration in 1000NMP(100ml)$^{-1}$,considering that the beginning of the y axis, is the point of the river mouth.

It was observed that the profiles of mean and maximum concentration, after some time do not change with time. The picture (11) shows the the behavior of concentration profiles given by the numerical model, for different times. In the picture (11) it is possible to see that the different profiles have a small variation, so the concentration reached a "almost steady" state.

The steady state profile it will be simulated by adjustments in analytical solutions presented on section 3. The solution are calibrated using an optimization algorithm.

The first step is to find a more convenient function to use in the algorithm. Imposing particular solutions in the solutions presented on section 2, we can construct expressions que describe diffusion-advection problems. The integral (16) have analytical solutions for a small number of cases. Besides, the analytical solutions generally are composed by expressions that are too "heavy" to run in the optimization algorithm. To deal with problems of computational time, we

Copyright © 2010 Asociación Argentina de Mecánica Computacional http://www.amcaonline.org.ar

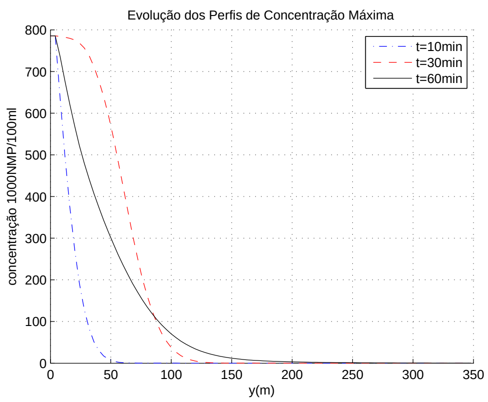

Figure 9: Maximum concentration of coliform on the surf zone along the coast in *t*=10 min, *t*=30 min and *t*=60 min

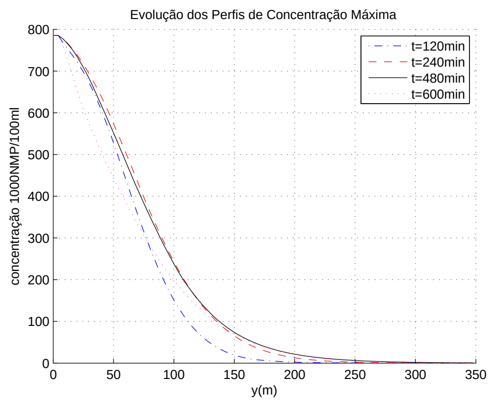

Figure 10: Maximum concentration of coliform on the surf zone along the coast in *t*=120 min, *t*=240 min ,*t*=480 min and *t*=600min

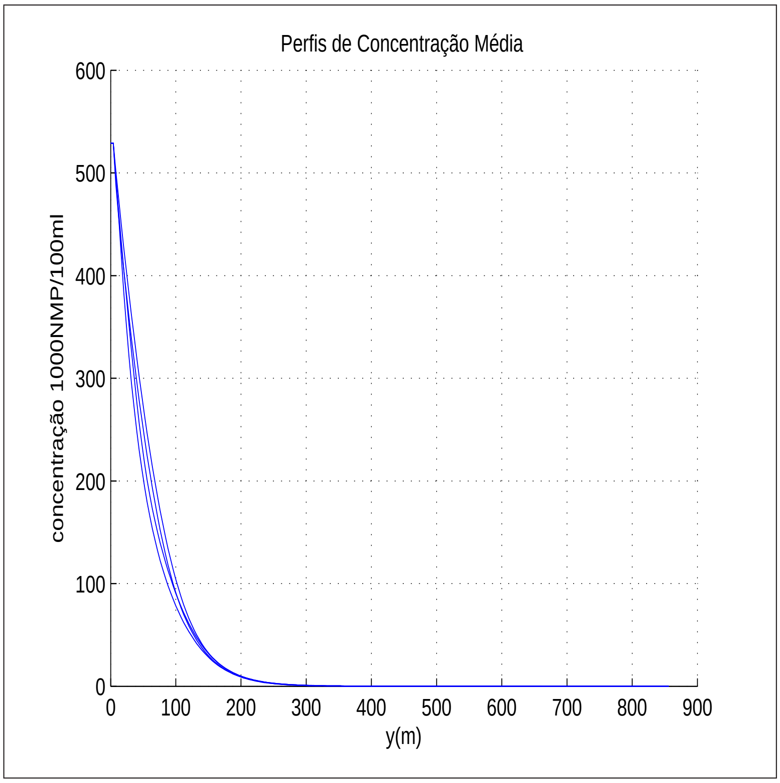

Figure 11: Steady state profile from the mean concentration

choose to use the expression (77).

5 CALIBRATION AND VALIDATION OF AN ANALYTICAL SOLUTION

The function (77) have the follow calibration parameters: C_0, D, V e K. Using the optimization algorithm it is possible to adjust the four parameters to minimize the difference between the steady state profile and the profile given by (77). The optimization algorithm used was the Sequential Quadratic Programming (SQP), that is described in details by Nocedal and Wright (1999) and Arora (2004). The function (77) was adjusted to fit the mean and maximum steady state profile in the surf zone. In both cases the initial values for the parameters D, V and K,

Copyright © 2010 Asociación Argentina de Mecánica Computacional http://www.amcaonline.org.ar

were the mean values calculated in the surf zone.

5.1 Adjustment for the steady state profile of the mean concentration of coliform in the surf zone

The table (1) shows the initial values and the intervals used for the calibration parameters in the optimization algorithm.

	C_0-NMP(100ml)$^{-1}$	D-m^{2}s^{-1}	V-ms^{-1}	K-s^{-1}
Valor inicial	529000	0,02	0,2	0,0002
Limite superior	600000	2	5	0,1
Limite inferior	0	0	0	0

Table 1: Initial values and the intervals used for the calibration parameters to fit the mean concentration

The values calculated by the algorithm were: $V = 0,6546$ ms^{-1}, $D = 2,5442$ m^{2}s^{-1}, $C_0 = 5742837$ NMP(100ml)$^{-1}$ e $K = 0,0070$ s^{-1}. The error from the analytical solution in respect to the concentration given by numerical simulation is $2,3\%$. The figure (12) shows the comparison between the numerical an analytical profiles.

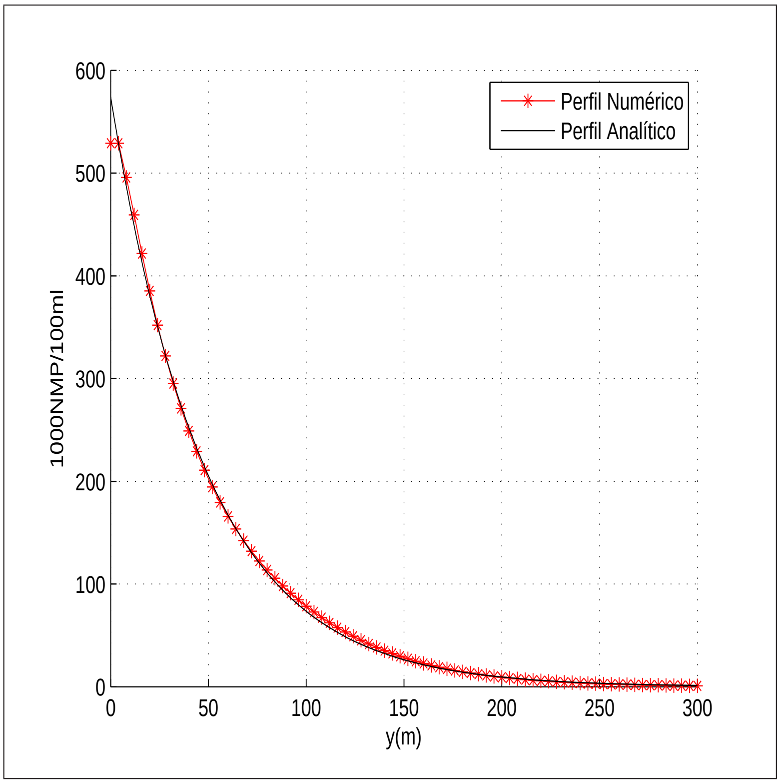

Figure 12: Comparison between the numerical and analytical profiles from the mean concentration of coliform in the surf zone

According to the policies of bathing of Paraná state, concentrations of coliform above 1000NMP(100ml)$^{-1}$ represents a water unfit to bathing. With this, a way to validate the calibrated functions is the capacite to predict the distance that the concentration reaches values above the critical limit. The analytical solution predicts that in 420 m the mean concentration would be below the critical limit. The numerical solution predicts 296 m to the same situation.

Copyright © 2010 Asociación Argentina de Mecánica Computacional http://www.amcaonline.org.ar

To obtain more accurate predictions by the analytical solution, we choose to disregard in the minimization, the regions close to the river mouth. So the algorithm only need to fit the numerical solution about 88 m from the river mouth. The values found were: $V = 0,6543$ ms^{-1}, $D = 2,5143$ m^{2}s^{-1}, $C_0 = 98922$ NMP(100ml)$^{-1}$ and $K = 0,0067$ s^{-1}. The error from the calibrated expression is $1,23$ percent. At this time, the analytical solutions predicts that in 320 m the mean concentration reaches the secure level. The error with respect to the numerical prediction is 24 meters. The figure (13)shows the comparison between the numerical and analytical profiles, starting in 88 meters from the river mouth.

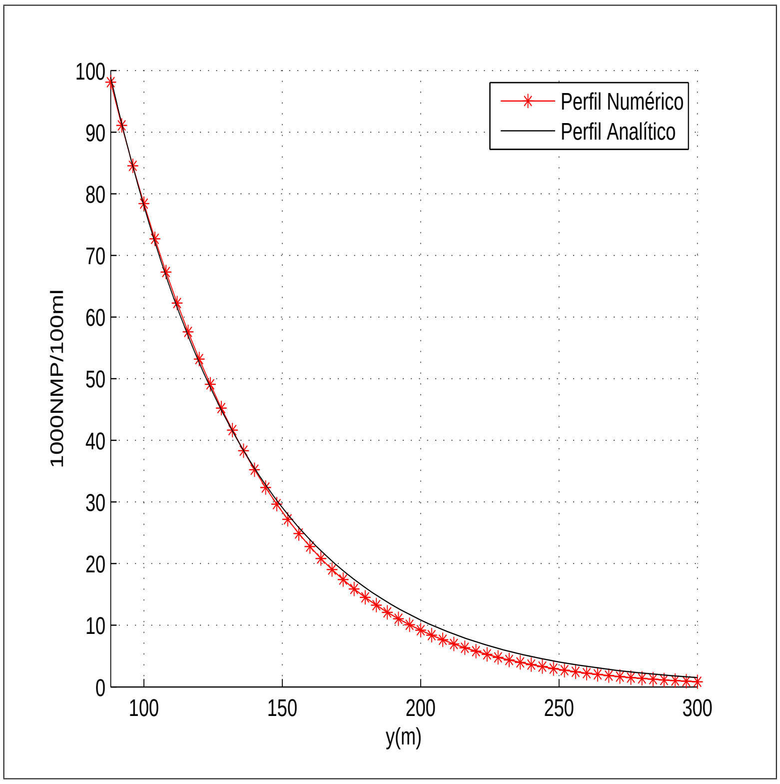

Figure 13: Comparison between the numerical and analytical partial profiles from the mean concentration of coliform in the surf zone

5.2 Adjustment for the steady state profile of the maximum concentration of coliform in the surf zone

For the adjustment of the analytical solution to the maximum concentration profile, the initial values used in to algorithm are described in table (1). The optimal values are: $V = 0,6582$ ms^{-1}, $D = 2,5290$ m^{2}s^{-1}, $C_0 = 851048$ NMP(100ml)$^{-1}$ and $K = 0,0045$ s^{-1}. The error from the analytical solution with respect to the numerical profile is $3,05\%$. The figure (14) shows the comparison between the numerical an analytical profiles of maximum concentration.

The analytical solution predicts that in 350 m the maximum concentration would be below the critical limit. The numerical solution predicts 336 m to the same situation. So the error for the prediction made by the analytical solution is 14 m.

Copyright © 2010 Asociación Argentina de Mecánica Computacional http://www.amcaonline.org.ar

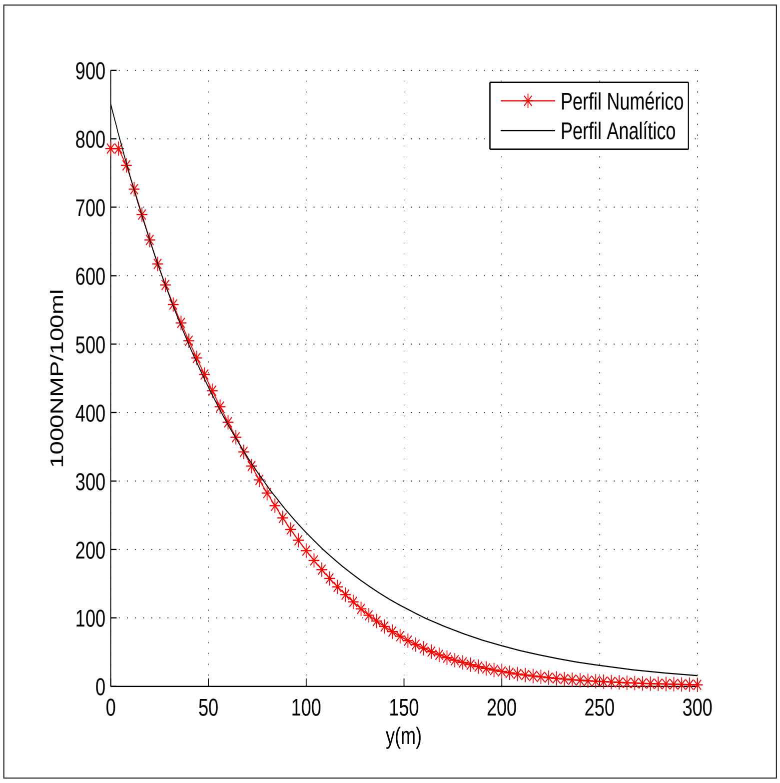

Figure 14: Comparison between the numerical and analytical profiles from the maximum concentration of coliform in the surf zone

6 CONCLUSION

It was possible to find a simple expression that had a low percentage of error, when it fits the behavior of coliform dispersion calculated by a numerical model with complex physical inputs.

The approach of using an optimization algorithm to calibrate the analytical function is satisfactory. But this approach becomes impracticable with the approximation function is too complex.

It was possible to find a simple analytical solution. The solutions presented in this paper are natural extensions of classical one-dimensional problems and they can by build using a good integral transform table. So the solutions presented in this paper has a good didactic potencial.

For an extension of this work it's possible to find more complex analytical solutions, as example: non-homogeneous velocity field and diffusion coefficient.

REFERENCES

Angulo R. As praias do paraná: problemas decorrentes de uma ocupação inadequada. *Boletim Analise Conjuntural*, 6:1–4, 1984.

Arora J. *Introduction to Optimum Design*. Elsevier, 2004.

Chen Q., Kennedy A., Kirby J., Dalrymple R., and Chawla A. Boussinesq modelling of wave transformation, breaking and runup. ii: Two horizonta dimensions. *Journal of Waterway, Port, Coastal and Ocean Engineering*, 126:39–47, 2000.

Figueiredo D. *Análise de Fourier e equações diferenciais parciais*, volume I. IMPA, 1977.

Kennedy A., Kirby J., Cheb Q., and Dalrymple R. Boussinesq modelling of wave transformation, breaking and runup. i: One dimension. *Journal of Waterway, Port, Coastal and Ocean Engineering*, 126:39–47, 2000.

Copyright © 2010 Asociación Argentina de Mecánica Computacional http://www.amcaonline.org.ar

Nocedal J. and Wright S. *Numerical Optimization*. Springer, 1999.

Solheid B. Dispersão de poluentes por ondas na zona de arrebentação. *Dissertação de mestrado*, 2010.

Wei G., Kirby J., and Subramanya R. A fully nonlinear boussinesq model for surface waves. i. highly nonlinear, unsteady waves. *Journal of fluid mechanics*, 294:71–92, 1995.

Copyright © 2010 Asociación Argentina de Mecánica Computacional http://www.amcaonline.org.ar